

Article

A Passively Q-Switched Holmium-Doped Fiber Laser with Graphene Oxide at 2058 nm

Jinho Lee and Ju Han Lee * 

School of Electronical and Computer Engineering, University of Seoul, Seoul 02504, Korea; wlsgh3124@uos.ac.kr
* Correspondence: jhl@uos.ac.kr; Tel.: +82-2-6490-2344

Abstract: This study reports a Q-switching-based, 2058-nm holmium (Ho) fiber laser incorporating a saturable absorber (SA) based on graphene oxide (GO). The SA was prepared with a side-polished fiber, while GO particles were deposited onto the fiber-polished surface to realize an all-fiber SA. A continuous-wave thulium-doped all-fiber laser, which was configured with a master-oscillator power-amplifier (MOPA) structure, was constructed as a pumping source. By inserting the fabricated SA into an all-fiber ring resonator based on 1-m length of Ho-doped fiber, Q-switched pulses could readily be obtained at a wavelength of 2058 nm. The pulse width was observed to vary from 2.01 to 1.56 μs as the pump power was adjusted from ~ 759 to 1072 mW, while the repetition rate was tunable from 45.56 to 56.12 kHz. The maximum values of average optical power and pulse energy were measured as ~ 11.61 mW and 207.05 nJ, respectively, at a ~ 1072 mW pump power.

Keywords: holmium-doped fiber; fiber laser; graphene oxide; saturable absorber; Q-switching



Citation: Lee, J.; Lee, J.H. A Passively Q-Switched Holmium-Doped Fiber Laser with Graphene Oxide at 2058 nm. *Appl. Sci.* **2021**, *11*, 407. <https://doi.org/10.3390/app11010407>

Received: 2 December 2020

Accepted: 29 December 2020

Published: 4 January 2021

Publisher's Note: MDPI stays neutral with regard to jurisdictional claims in published maps and institutional affiliations.



Copyright: © 2021 by the authors. Licensee MDPI, Basel, Switzerland. This article is an open access article distributed under the terms and conditions of the Creative Commons Attribution (CC BY) license (<https://creativecommons.org/licenses/by/4.0/>).

1. Introduction

Q-switched lasers operating at the $\sim 2\text{-}\mu\text{m}$ spectral region are attractive coherent light sources for numerous applications such as medicine, LiDAR, material processing, and gas sensing [1–4]. Compared with other types of lasers, fiber lasers have a range of benefits like low heat accumulation, environmental stability, alignment-free operation, and compactness [5]. Depending on the requirement of an external electrical signal source, Q-switched fiber lasers can be categorized into two groups: passive and active. Active Q-switching technique is commonly used in most of commercial products of pulsed fiber lasers with output pulse widths from nanoseconds to microseconds, due to its features of a high energy output and a controllable pulse repetition rate. Comparatively speaking, passive Q-switching technique is still of intensive research interest due to its future potential associated with a simple configuration that does not require an external modulator.

One of the common approaches to implement passive Q-switching in a rare-earth-doped fiber-based laser configuration is to incorporate a passive device with a function of saturable absorption into a laser resonator. This type of a passive device is called “saturable absorber (SA)”. Until now, III-V-compound semiconducting materials have been used for commercial-grade SAs and such commercial-grade SAs were successfully employed for generating Q-switched pulses from a laser cavity [6]. However, various limitations were found for the SAs based on III-V-compound semiconducting materials and the limitations include the essential requirement of high-cost, clean-room fabrication facilities and the narrow operating bandwidth. For the purpose of overcoming the issues related to the SAs based on III-V-compound semiconducting materials, intensive investigations have been conducted to find material substitutes. Until now, a range of promising candidates have been reported and those materials include carbon nanotubes (CNTs) [7–11], graphene [12], graphene oxide (GO) [13,14], topological insulators (TIs) [15–22], transition metal dichalcogenides (TMDCs) [23–32], transition metal monochalcogenides (TMMCs) [33], black phosphorus (BPs) [34–36], gold nano particles [37–39], chromium-doped fiber [40], and MXenes [41,42].

Among the aforementioned nonlinear absorption materials, graphene has been regarded as highly promising for high-performance devices in the field of photonics owing to its distinct and outstanding characteristics, such as its no energy bandgap structure, high carrier mobility, fast relaxation, large optical third-order nonlinearity, and optical transparency over a wide spectral band region [43,44]. Therefore, graphene has proven to be useful in many photonic applications such as four wave-mixing [45], optical modulators [46], polarizers [47], and SAs [48–52]. In particular, the use of graphene for the realization of SAs has received significant attention due to its inherent advantages of fast recovery time, large operating bandwidth, and high optical damage threshold. Since Bao et al. first reported that graphene could be used as an effective SA material in 2009 [12], the graphene-based SAs have been intensively investigated for their application to passively mode-locked or Q-switched lasers at various wavelengths [48–52]. Apart from graphene, GO and reduced GO, which are low-cost variations from graphene have also been investigated in terms of saturable absorption [13,14,53,54].

In general, fiber lasers operating in the wavelength band from 1.9 to 2.1 μm can be realized using thulium (Tm)-doped fiber, thulium-holmium (Tm-Ho) codoped fiber, or holmium (Ho)-doped fiber as a gain medium. It should be noticed that a Tm-doped fiber cavity generates a pulsed laser output at around 1.9- μm wavelengths, whereas a Ho-doped fiber cavity does so at around 2 μm . Until now, most of the investigations in short pulse generation in the wavelength band from 1.9 to 2.1 μm have been focused on the use of a Tm-doped fiber cavity due to easy availability of semiconductor pumping sources at ~ 0.79 and ~ 1.56 μm [55–58]. Ho-doped silica fiber produces photon emission over a wavelength region of 2.05–2.17 μm [59] and is pumped by laser sources operating at ~ 1.1 and ~ 1.9 μm . One should note that semiconductor-based pump sources are not easily available at wavelengths of ~ 1.1 and ~ 1.9 μm [60–62]. Until now, there have been quite a few reports on Ho-doped fiber-based pulsed lasers, and they were based on various pulse formation techniques such as gain-switching [63–65], nonlinear polarization rotation (NPR) [66], and saturable absorption [67]. It should be noted that the previous works on Ho-doped fiber-based pulsed lasers mostly focused on mode-locked pulse generation with various nonlinear saturable absorption materials, such as CNTs [67,68], graphene [69,70], and BP [71]; however, only a few investigations have been reported with respect to Q-switched pulse generation from a Ho-doped fiber cavity with an SA [72–75]. More specifically, Chamorovskiy et al. demonstrated a Q-switched Ho-doped fiber laser incorporating a CNT-based SA [72], Sholokhov et al. reported a Q-switched Ho-doped fiber laser with a heavily Ho-doped fiber SA [74], and Wang et al. demonstrated the use of a heavily Ho-doped fiber SA for the realization of high-power Q-switched pulses from a Ho-doped fiber laser [75].

In this work, a Q-switched Ho-doped fiber laser using a low-cost SA based on GO is experimentally demonstrated. The SA, which has an all-fiber structure, was implemented through deposition of GO particles onto the flat polished surface of a side-polished fiber. In order to pump a Ho-doped fiber gain medium in the laser ring resonator, our built continuous-wave (CW) Tm-doped fiber laser at 1928 nm, which was followed by a power amplifier operating was used. By inserting the GO-based SA in the prepared Ho-doped fiber-based ring resonator, the pulsed output was found to be readily obtainable at a wavelength of 2058 nm due to passive Q-switching. The measured temporal width of the output pulses was 1.56 μs at a 56.12 kHz repetition rate. Both output pulse width and repetition were tunable by changing the pump power. It should be noticed that this study's constructed laser has an all-fiber ring configuration unlike the Q-switching-based Ho-doped fiber laser incorporating a SA based on CNT, demonstrated by Chamorovskiy et al. in which a Fabry-Pérot cavity was employed with a free-space coupled mirror-type SA [72]. The main goal of this work is to demonstrate the ultimate potential of graphene oxide (GO) as a base material for the implementation of our SA since it is a low-cost alternative to expensive high-purity graphene in terms of saturable absorption. Note that GO-based SAs have not been used for passive Q-switching of a fiber laser operating at the

wavelength band beyond 2 μm , even if they have been well-investigated at wavelengths of 1, 1.5, and 1.9 μm .

2. Characterization and Preparation of the GO-Based Saturable Absorber

The conventional, low-cost GO was obtained from a commercial company for this experimental demonstration. The measured Raman spectrum of the GO particles is illustrated in Figure 1a. The D band and G band were observed at 1348 and 1592 cm^{-1} , each. The D peak is known to be induced by the lattice disorder of graphene [76], while the G peak is caused by the phonon excitation at the Brillouin zone center [77]. The X-ray photoelectron spectroscopy (XPS) spectrum was also measured and the spectrum in the C 1s region of the GO particles is shown in Figure 1b. After curve fitting, it was found that the fitted C 1s peaks could be decomposed by three peaks at ~ 284.8 , ~ 286.7 , and ~ 287.9 eV, which correspond to groups of C-C/C=C, C-O, and C=O, respectively. These peaks correspond to those of the previously reported values [78].

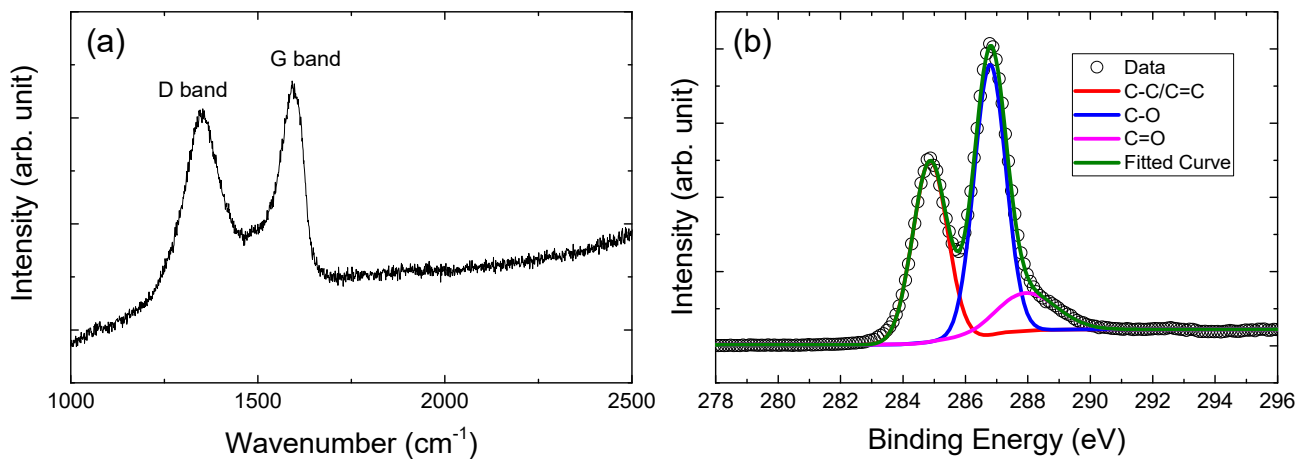


Figure 1. (a) Raman spectrum and (b) XPS spectrum (C 1s) of the graphene oxide (GO) particles.

Figure 2a illustrates the linear optical absorption spectrum for the GO particles, which was measured with a spectrophotometer. The linear absorption spectrum indicates that the GO particles have a broad absorption band that include the 2.0–2.1 μm regime. A schematic diagram of the GO-deposited side-polished fiber is shown in Figure 2b. One side of a standard single-mode fiber (SMF) was finely polished to obtain a side-polished fiber, which enables us to induce evanescent field interaction with the deposited GO particles. The physical distance between the polished surface and core edge was ~ 5 μm . The polished length of the fiber was ~ 3 mm, and the length covered with GO was ~ 8 mm. The used GO has a single layer with a thickness of ~ 500 nm. Note that the used GO has no atomic layer structure. The insertion loss (IL) of the side-polished fiber was ~ 0.7 dB and its polarization-dependent loss (PDL) was ~ 0.04 dB. After the GO particles were deposited onto the polished surface, the IL was changed into ~ 2.8 dB, while the PDL became ~ 3.4 dB.

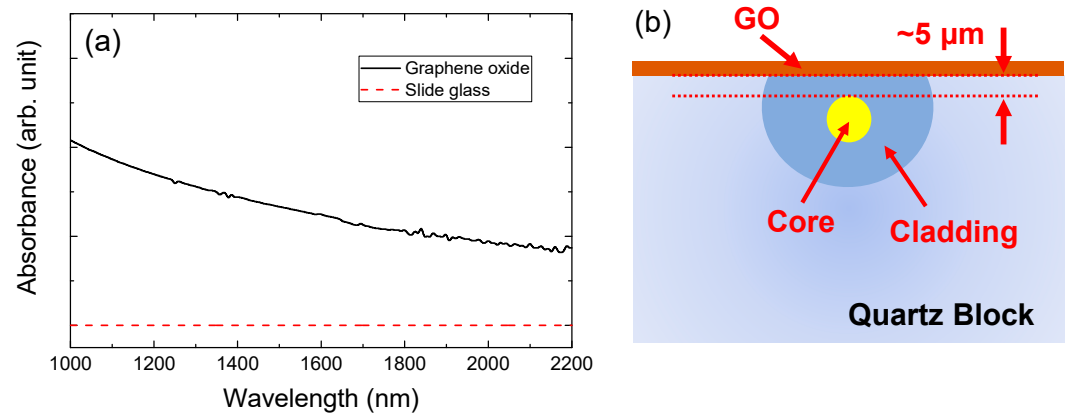


Figure 2. (a) Linear optical absorption spectrum of the GO particles. (b) Schematic diagram of GO-deposited side-polished fiber.

Next, nonlinear transmission measurement was performed as a function of the input pulse peak power for the fabricated GO-deposited SA, using an experimental setup in Figure 3a. The incident beam was coupled into the GO-based SA in the transverse electric (TE) mode. For this measurement, we used a passively mode-locked fiber laser with a repetition rate of ~ 36.94 MHz and a temporal width of ~ 711 fs at 1902 nm. Since an ultrafast laser source operating at a $2.0\text{--}2.1\text{-}\mu\text{m}$ wavelength region did not exist in our laboratory, this particular measurement was carried out at $1.9\ \mu\text{m}$ with our built mode-locked Tm-doped fiber laser. The nonlinear transmission curve of the GO-based SA, is illustrated in Figure 3b together with its corresponding fitting curve [79]:

$$T(I) = 1 - \Delta T \cdot \exp\left(\frac{-I}{I_{sat}}\right) - T_{ns}, \quad (1)$$

where $T(I)$ and ΔT are the transmission and modulation depth, respectively. I and I_{sat} are the input-pulse energy and saturation energy, respectively. T_{ns} represents the nonsaturable loss. The modulation depth and saturation power were estimated at $\sim 13.1\%$ and ~ 12.5 W, respectively.

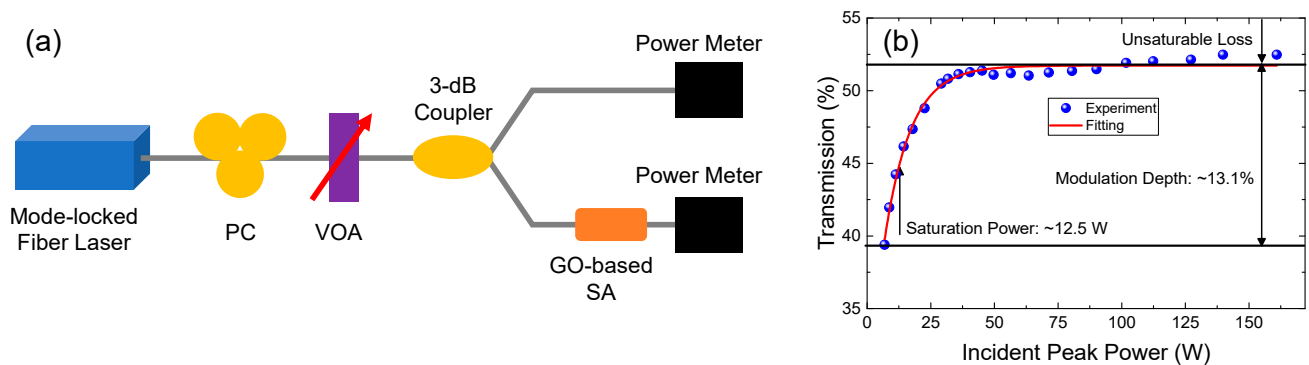


Figure 3. (a) Measurement setup for nonlinear transmission curve. (b) Measured nonlinear transmission curve of the prepared GO-based saturable absorber (SA). (PC: polarization controller, VOA: variable optical attenuator).

3. Q-Switching of a 2058-nm Fiber Laser

The whole laser schematic diagram including a Ho-doped fiber ring resonator and a Tm-doped fiber-based high power pumping source is presented in Figure 4. Our laser was constructed with single-clad Ho-doped fiber rather than double clad one, since our targeted laser did not require a high output power. We chose a 1900-nm Tm-doped fiber laser as a pumping source for the Ho-doped fiber considering the fact that the pump absorption based on the transition of ${}^5I_8 \rightarrow {}^5I_7$ allows for better quantum efficiency than

that of $^5I_8 \rightarrow ^5I_6$ [80]. Taking into account that our prepared SA had a transmission type configuration, our laser cavity was constructed with a simple ring structure. The all-fiber continuous-wave (CW) thulium-doped master oscillator and power amplifier (MOPA) source consists of a CW seed oscillator, a Tm-Ho-codoped fiber prestage amplifier, and a Tm-doped fiber main-amplifier. The output beam from the seed oscillator was first amplified with a preamplifier stage and then further amplified with a main power amplifier stage. The output wavelength of the CW seed oscillator was ~ 1928 nm. The output of the seed oscillator was coupled into a preamplifier stage via a 1550/2000-nm wavelength division multiplexer (WDM). For the prestage amplifier, 1-m length of Tm-Ho-codoped fiber an absorption of 13 dB/m at 1550 nm was used. A commercially available 1550 nm erbium-doped fiber amplifier (EDFA) was used as a pumping source for the prestage amplifier. The main stage amplifier was comprised a 793 nm laser diode (LD), a $(2 + 1) \times 1$ combiner, and 3-m length of double-clad (DC) Tm-doped fiber. The cladding absorption of the DC-Tm-doped fiber at 793 nm was ~ 4.5 dB/m. The core and inner cladding diameter were 10 and 130 μm , respectively. The 1928-nm pumping beam, which had a maximum power of ~ 1.1 W was launched into the Ho-doped fiber ring resonator through a 1930/2080-nm WDM. A 1-m-long Ho-doped fiber (Nufern SM-HDF-10/130) was used as a gain medium for the cavity. To ensure unidirectional light propagation, an isolator was used. A 90:10 output coupler was utilized to extract the laser output, and the output pulses were obtained from the 10% port through a 90:10 coupler.

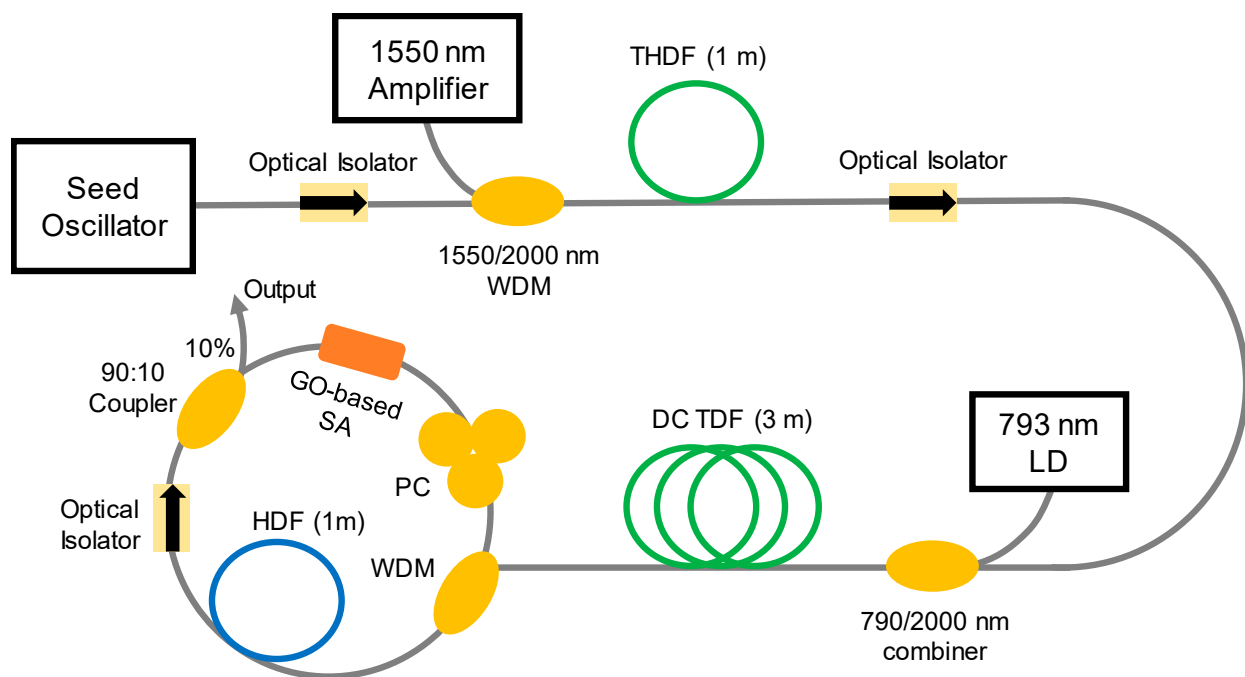


Figure 4. Experimental setup of the Q-switched, holmium-doped fiber laser. (THDF: thulium-holmium co-doped fiber, DC TDF: double-clad thulium-doped fiber, HDF: holmium-doped fiber, PC: polarization controller, WDM: wavelength division multiplexer).

In order to induce lasing from the all-fiber resonator, the pump power was enlarged. The CW lasing was observed to start when the pump power reached ~ 660 mW. Subsequently, the CW lasing mode was converted into the Q-switching mode as soon as the pump power arrived at ~ 759 mW. The measured optical spectrum of the Q-switched pulses at a pump power of ~ 759 mW is shown in Figure 5a. The peak wavelength was ~ 2058 nm and interestingly, multiple peaks were observed in the optical spectrum, implying that gain competition among many longitudinal modes occurred, such longitudinal mode instabilities in fiber laser devices were reviewed in [81,82]. This intermode gain competition can be associated with the fact that no mode-selective filtering component was used in the

laser configuration. Figure 5b illustrated the output oscilloscope traces at various pump power levels. It is clearly evident that stable Q-switching operation were maintained over a wide range of pump powers above the threshold of ~ 759 mW. The temporal period of the output pulses was observed to decrease when the pump beam power became larger. This sort of pulse temporal behavior depending on pump power is a typical phenomenon, which is generally reported in passively Q-switched fiber lasers using an SA [16,24,35].

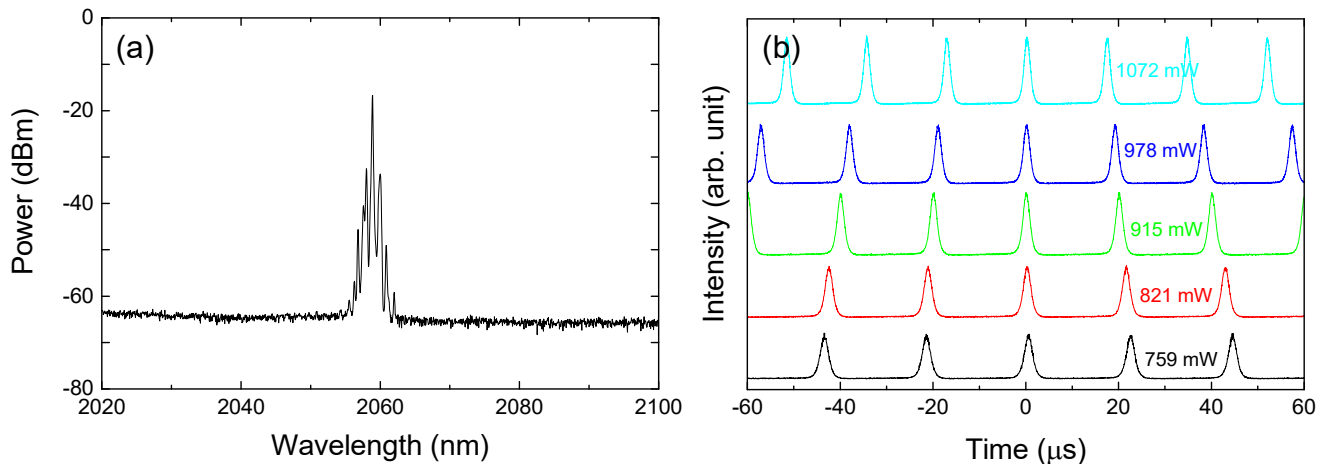


Figure 5. (a) Measured optical spectrum of the output pulses at pump power of 759 mW. (b) Measured oscilloscope traces of the output pulses at a variety of pump powers.

Subsequently, the average optical power, pulse energy, and repetition rate of the output pulses were monitored while changing the pump power. The results are illustrated in Figure 6. The pulse width decreased from 2.01 to 1.56 μs as the pump power was adjusted from ~ 759 to 1072 mW, while the repetition rate changed from 45.56 to 56.12 kHz, as shown in Figure 6a. The pump power-dependent pulse width change could be attributed to the pump-induced gain compression effect [16,35,83]. The pulse energy as well as the average output power was observed to increase as the pump power was enlarged, as shown in Figure 6b. The maximum values of pulse energy and average output power were ~ 11.62 mW and 207.05 nJ, respectively, each at the maximum pump power of ~ 1072 mW. Finally, a performance comparison between previously demonstrated Q-switched Ho-doped fiber lasers with SAs and our laser is presented in the Table 1. It is obvious from the table that our laser exhibited better performance than the laser using a CNT-based SA in terms of pulse energy. From a perspective of pulse energy scalability, the Ho-doped fiber SA is the best among the three due to its high damage threshold. Apparently, nanomaterial-based SAs have damage threshold issues, which are critical to obtaining high energy pulses directly from a laser cavity.

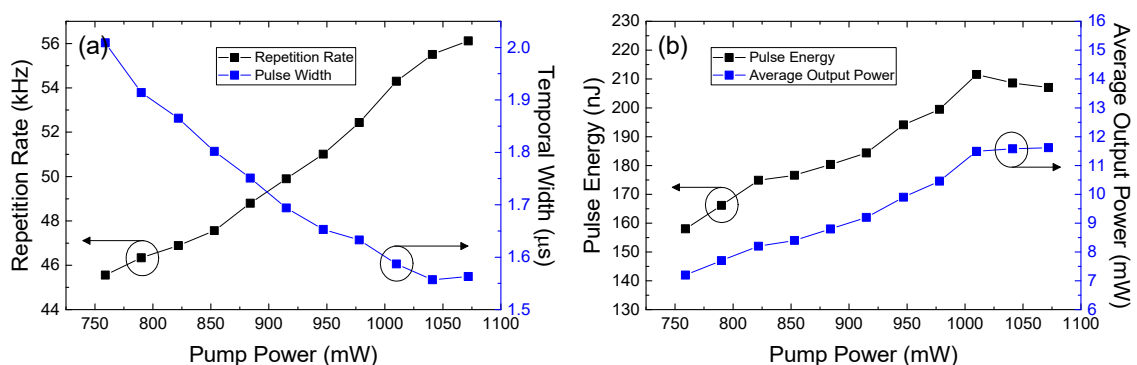


Figure 6. (a) Measured repetition rate and temporal width of the output pulses as a function of the pump power. (b) Measured pulse energy and average output power of the output pulses as a function of the pump power.

Table 1. Performance comparison between previously demonstrated Q-switched Ho-doped fiber lasers with saturable absorber (SAs) and our laser.

SAs	Center Wavelength (nm)	Max. Repetition Rate (kHz)	Min. Pulse Width (μ s)	Max. Pulse Energy (nJ)	Reference
CNT	2097	170	0.32	118	[72]
Ho-fiber	2050	190	0.45	7000	[74]
GO	2058	56.12	1.56	207.05	This work

4. Conclusions

A passively Q-switched 2058 nm laser with an all-fiber configuration incorporating a GO-based SA has been experimentally demonstrated in this study. The all-fiber SA was fabricated with GO particles deposited onto the polished side surface of a standard optical fiber. It was discovered that stable microsecond pulses could be generated at 2058 nm when the prepared SA was inserted into a ring resonator incorporating a Ho-doped fiber gain medium. The minimum pulse width was $\sim 1.56 \mu$ s at a ~ 1072 mW pump power.

These experimental results are believed to be a useful part of a database of pulsed Ho-doped fiber lasers, which have not been extensively investigated until now.

Author Contributions: Conceptualization, J.L. and J.H.L.; methodology, J.L.; validation, J.L. and J.H.L.; formal analysis, J.L. and J.H.L.; investigation, J.L.; resources, J.L.; data curation, J.L.; writing—original draft preparation, J.L.; writing—review and editing, J.H.L.; visualization, J.L. All authors have read and agreed to the published version of the manuscript.

Funding: This work was supported by the 2020 Research Fund of the University of Seoul.

Institutional Review Board Statement: Not applicable.

Informed Consent Statement: Not applicable.

Data Availability Statement: Data sharing not applicable.

Conflicts of Interest: The authors declare no conflict of interest.

References

- De Young, R.J.; Barnes, N.P. Profiling atmospheric water vapor using a fiber laser lidar system. *Appl. Opt.* **2010**, *49*, 562–567. [[CrossRef](#)] [[PubMed](#)]
- McAleavey, F.J.; O’Gorman, J.; Donegan, J.F.; MacCraith, B.D.; Hegarty, J.; Maze, G. Narrow linewidth, tunable Tm/sup 3+/-doped fluoride fiber laser for optical-based hydrocarbon gas sensing. *IEEE J. Sel. Top. Quantum Electron.* **1997**, *3*, 1103–1111. [[CrossRef](#)]
- Todorov, F.; Aubrecht, J.; Peterka, P.; Schreiber, O.; Jasim, A.A.; Mrázek, J.; Podrazký, O.; Kamrádek, M.; Kanagaraj, N.; Grábner, M.; et al. Active optical fibers and components for fiber lasers emitting in the 2- μ m spectral range. *Materials* **2020**, *13*, 5177. [[CrossRef](#)] [[PubMed](#)]
- Fried, N.M.; Murray, K.E. High-Power Thulium Fiber Laser Ablation of Urinary Tissues at 1.94 μ m. *J. Endourol.* **2005**, *19*, 25–31. [[CrossRef](#)]
- Richardson, D.J.; Nilsson, J.; Clarkson, W.A. High power fiber lasers: Current status and future perspectives [Invited]. *J. Opt. Soc. Am. B* **2010**, *27*, B63–B92. [[CrossRef](#)]
- Keller, U.; Weingarten, K.; Kartner, F.X.; Kopf, D.; Braun, B.; Jung, I.; Fluck, R.; Honninger, C.; Matuschek, N.; Der Au, J.A. Semiconductor saturable absorber mirrors (SESAM’s) for femtosecond to nanosecond pulse generation in solid-state lasers. *IEEE J. Sel. Top. Quantum Electron.* **1996**, *2*, 435–453. [[CrossRef](#)]
- Set, S.Y.; Yaguchi, H.; Tanaka, Y.; Jablonski, M. Laser Mode Locking Using a Saturable Absorber Incorporating Carbon Nanotubes. *J. Light. Technol.* **2004**, *22*, 51–56. [[CrossRef](#)]
- Yamashita, S.; Inoue, Y.; Maruyama, S.; Murakami, Y.; Yaguchi, H.; Jablonski, M.; Set, S.Y. Saturable absorbers incorporating carbon nanotubes directly synthesized onto substrates and fibers and their application to mode-locked fiber lasers. *Opt. Lett.* **2004**, *29*, 1581–1583. [[CrossRef](#)]
- Wang, F.; Rozhin, A.G.; Scardaci, V.; Sun, Z.; Hennrich, F.; White, I.H.; Milne, W.I.; Ferrari, A.C. Wideband-tuneable, nanotube mode-locked, fibre laser. *Nat. Nanotechnol.* **2008**, *3*, 738–742. [[CrossRef](#)]
- Martinez, A.; Sun, Z. Nanotube and graphene saturable absorbers for fibre lasers. *Nat. Photon.* **2013**, *7*, 842–845. [[CrossRef](#)]

11. Weigand, R.; Balmaseda, M.S.; Guerra, J.M. Q-Switched Operation with Carbon-Based Saturable Absorbers in a Nd:YLF Laser. *Appl. Sci.* **2015**, *5*, 566–574. [[CrossRef](#)]
12. Bao, Q.; Zhang, H.; Wang, Y.; Ni, Z.; Yan, Y.; Shen, Z.; Loh, K.P.; Tang, D.Y. Atomic-Layer Graphene as a Saturable Absorber for Ultrafast Pulsed Lasers. *Adv. Funct. Mater.* **2009**, *19*, 3077–3083. [[CrossRef](#)]
13. Liu, C.; Ye, C.; Luo, Z.; Cheng, H.; Wu, D.; Zheng, Y.; Liu, Z.; Qu, B. High-energy passively Q-switched 2 μm Tm³⁺-doped double-clad fiber laser using graphene-oxide-deposited fiber taper. *Opt. Express* **2013**, *21*, 204–209. [[CrossRef](#)] [[PubMed](#)]
14. Jung, M.; Koo, J.; Park, J.; Song, Y.-W.; Jhon, Y.M.; Lee, K.; Lee, S.; Lee, J.H. Mode-locked pulse generation from an all-fiberized, Tm-Ho-codoped fiber laser incorporating a graphene oxide-deposited side-polished fiber. *Opt. Express* **2013**, *21*, 20062–20072. [[CrossRef](#)] [[PubMed](#)]
15. Zhao, C.; Zhang, H.; Qi, X.; Chen, Y.; Wang, Z.; Wen, S.; Tang, D. Ultra-short pulse generation by a topological insulator based saturable absorber. *Appl. Phys. Lett.* **2012**, *101*, 211106. [[CrossRef](#)]
16. Luo, Z.; Liu, C.; Huang, Y.; Wu, D.; Wu, J.; Xu, H.; Cai, Z.; Lin, Z.; Sun, L.; Weng, J. Topological-insulator passively Q-switched double-clad fiber laser at 2 μm wavelength. *IEEE J. Sel. Top. Quantum Electron.* **2014**, *20*, 0902708.
17. Jung, M.; Lee, J.; Koo, J.; Park, J.; Song, Y.-W.; Lee, K.; Lee, S.; Lee, J.H. A femtosecond pulse fiber laser at 1935 nm using a bulk-structured Bi₂Te₃ topological insulator. *Opt. Express* **2014**, *22*, 7865–7874. [[CrossRef](#)]
18. Lin, Y.-H.; Lin, S.-F.; Chi, Y.-C.; Wu, C.-L.; Cheng, C.-H.; Tseng, W.-H.; He, J.-H.; Wu, C.-I.; Lee, C.-K.; Lin, G.-R. Using n- and p-Type Bi₂Te₃ Topological Insulator Nanoparticles to Enable Controlled Femtosecond Mode-Locking of Fiber Lasers. *ACS Photon.* **2015**, *2*, 481–490. [[CrossRef](#)]
19. Boguslawski, J.; Sobon, G.; Tarnowski, K.; Zybala, R.; Mars, K.; Mikula, A.; Abramski, K.M.; Sotor, J. All-polarization-maintaining-fiber laser Q-switched by evanescent field interaction with Sb₂Te₃ saturable absorber. *Opt. Eng.* **2016**, *55*, 81316. [[CrossRef](#)]
20. Jhon, Y.I.; Lee, J.; Jhon, J.M.; Lee, J.H. Topological insulator for mode-locking of 2- μm fiber lasers. *IEEE J. Sel. Top. Quantum Electron.* **2018**, *24*, 1102208. [[CrossRef](#)]
21. Qiao, J.; Zhao, S.; Yang, K.; Song, W.-H.; Qiao, W.; Wu, C.-L.; Zhao, J.; Li, G.; Li, D.; Li, T.; et al. High-quality 2- μm Q-switched pulsed solid-state lasers using spin-coating-coreduction approach synthesized Bi₂Te₃ topological insulators. *Photon. Res.* **2018**, *6*, 314–320. [[CrossRef](#)]
22. Lee, J.; Kim, T.; Lee, J.H. Investigation into nonlinear optical absorption property of CoSb₃ skutterudite in the 2 μm spectral region. *Opt. Laser Technol.* **2020**, *129*, 106274. [[CrossRef](#)]
23. Zhang, H.; Lu, S.B.; Zheng, J.; Du, J.; Wen, S.C.; Tang, D.Y.; Loh, K.P. Molybdenum disulfide (MoS₂) as a broadband saturable absorber for ultra-fast photonics. *Opt. Express* **2014**, *22*, 7249–7260. [[CrossRef](#)] [[PubMed](#)]
24. Luan, C.; Zhang, X.; Yang, K.; Zhao, J.; Zhao, S.; Li, T.; Qiao, W.; Chu, H.; Qiao, J.; Wang, J.; et al. High-Peak Power Passively Q-Switched 2- μm Laser with MoS₂ Saturable Absorber. *IEEE J. Sel. Top. Quantum Electron.* **2016**, *23*, 66–70. [[CrossRef](#)]
25. Mao, D.; Wang, Y.; Ma, C.; Han, L.; Jiang, B.; Gan, X.; Hua, S.; Zhang, W.; Mei, T.; Zhao, J. WS₂ mode-locked ultrafast fiber laser. *Sci. Rep.* **2015**, *5*, srep07965. [[CrossRef](#)]
26. Yang, Y.-Y.; Yang, S.; Li, C.; Lin, X. Passively Q-switched and mode-locked Tm-Ho co-doped fiber laser using a WS₂ saturable absorber fabricated by chemical vapor deposition. *Opt. Laser Technol.* **2019**, *111*, 571–574. [[CrossRef](#)]
27. Woodward, R.I.; Howe, R.C.T.; Runcorn, T.H.; Hu, G.; Torrisi, F.; Kelleher, E.J.R.; Hasan, T. Wideband saturable absorption in few-layer molybdenum diselenide (MoSe₂) for Q-switching Yb-, Er- and Tm-doped fiber lasers. *Opt. Express* **2015**, *23*, 20051–20061. [[CrossRef](#)]
28. Lee, J.; Koo, J.; Lee, J.; Jhon, Y.M.; Lee, J.H. All-fiberized, femtosecond laser at 1912 nm using a bulk-like MoSe₂ saturable absorber. *Opt. Mater. Express* **2017**, *7*, 2968–2979. [[CrossRef](#)]
29. Wang, J.; Xu, Z.; Liu, W.-J.; Yan, P.; Lu, W.; Li, J.; Chen, H.; Jiang, Z.; Wang, J.; Zhang, W.; et al. Ultrafast Thulium-Doped Fiber Laser Mode Locked by Monolayer WSe₂. *IEEE J. Sel. Top. Quantum Electron.* **2018**, *24*, 1–6. [[CrossRef](#)]
30. Mao, D.; Du, B.; Xiaoyang, S.; Zhang, S.; Wang, Y.; Zhang, W.; Shengli, Z.; Cheng, H.; Zeng, H.; Zhao, J. Nonlinear Saturable Absorption of Liquid-Exfoliated Molybdenum/Tungsten Ditelluride Nanosheets. *Small* **2016**, *12*, 1489–1497. [[CrossRef](#)]
31. Mao, D.; Cui, X.; Gan, X.; Li, M.; Zhang, W.; Lu, H.; Zhao, J. Passively Q-switched and mode-locked fiber laser based on an ReSe₂ saturable absorber. *IEEE J. Sel. Top. Quantum Electron.* **2018**, *24*, 1100406. [[CrossRef](#)]
32. Lee, J.; Lee, K.; Kwon, S.; Shin, B.; Lee, J.H. Investigation of nonlinear optical properties of rhenium diselenide and its application as a femtosecond mode-locker. *Photon Res.* **2019**, *7*, 984–993. [[CrossRef](#)]
33. Jhon, Y.I.; Lee, J.; Seo, M.; Lee, J.H.; Jhon, Y.M. van der Waals layered tin selenide as highly nonlinear ultrafast saturable absorber. *Adv. Opt. Mater.* **2019**, *7*, 1801745. [[CrossRef](#)]
34. Chen, Y.; Jiang, G.; Chen, S.; Guo, Z.; Yu, X.; Zhao, C.; Zhang, H.; Bao, Q.; Wen, S.; Tang, D.; et al. Mechanically exfoliated black phosphorus as a new saturable absorber for both Q-switching and Mode-locking laser operation. *Opt. Express* **2015**, *23*, 12823–12833. [[CrossRef](#)] [[PubMed](#)]
35. Yu, H.; Zheng, X.; Yin, K.; Cheng, X.; Jiang, T. Nanosecond passively Q-switched thulium/holmium-doped fiber laser based on black phosphorus nanoplatelets. *Opt. Mater. Express* **2016**, *6*, 603–609. [[CrossRef](#)]
36. Sotor, J.; Sobon, G.; Macherzynski, W.; Paletko, P.; Abramski, K.M. Black phosphorus saturable absorber for ultrashort pulse generation. *Appl. Phys. Lett.* **2015**, *107*, 051108. [[CrossRef](#)]
37. Jiang, T.; Xu, Y.; Tian, Q.; Liu, L.; Kang, Z.; Yang, R.; Qin, G.; Qin, W. Passively Q-switching induced by gold nanocrystals. *Appl. Phys. Lett.* **2012**, *101*, 151122. [[CrossRef](#)]

38. Kang, Z.; Liu, M.Y.; Gao, X.J.; Li, N.; Yin, S.Y.; Qin, G.S.; Qin, W.P. Mode-locked thulium-doped fiber laser at 1982 nm by using a gold nanorods saturable absorber. *Laser Phys. Lett.* **2015**, *12*, 045105. [[CrossRef](#)]
39. Lee, J.; Koo, J.; Lee, J.; Lee, J.H. End-to-end self-assembly of gold nanorods in water solution for absorption enhancement at a 1-to-2 μm band for a broadband saturable absorber. *J. Lightwave Technol.* **2016**, *34*, 5250–5257. [[CrossRef](#)]
40. Dussardier, B.; Maria, J.; Peterka, P. Passively Q-switched ytterbium- and chromium-doped all-fiber laser. *Appl. Opt.* **2011**, *50*, E20–E23. [[CrossRef](#)]
41. Jhon, Y.I.; Koo, J.; Anasori, B.; Seo, M.; Lee, J.H.; Gogotsi, Y.; Jhon, Y.M. Metallic MXene saturable absorber for femtosecond mode-locked lasers. *Adv. Mater.* **2017**, *29*, 1702496. [[CrossRef](#)] [[PubMed](#)]
42. Jiang, X.; Liu, S.; Liang, W.; Luo, S.; He, Z.; Ge, Y.; Wang, H.; Cao, R.; Zhang, F.; Wen, Q.; et al. Broadband Nonlinear Photonics in Few-Layer MXene $\text{Ti}_3\text{C}_2\text{T}_x$ ($T = \text{F}, \text{O}, \text{or OH}$). *Laser Photon. Rev.* **2018**, *12*, 1700229. [[CrossRef](#)]
43. Bonaccorso, F.; Sun, Z.; Hasan, T.; Ferrari, A.C. Graphene photonics and optoelectronics. *Nat. Photon.* **2010**, *4*, 611–622. [[CrossRef](#)]
44. Avouris, P.; Freitag, M. Graphene Photonics, Plasmonics, and Optoelectronics. *IEEE J. Sel. Top. Quantum Electron.* **2013**, *20*, 72–83. [[CrossRef](#)]
45. Hendry, E.; Hale, P.J.; Moger, J.J.; Savchenko, A.K.; Mikhailov, S.A. Coherent Nonlinear Optical Response of Graphene. *Phys. Rev. Lett.* **2010**, *105*, 097401. [[CrossRef](#)] [[PubMed](#)]
46. Liu, M.; Yin, X.; Ulin-Avila, E.; Geng, B.; Zentgraf, T.; Ju, L.; Wang, F.; Zhang, X. A graphene-based broadband optical modulator. *Nat. Cell Biol.* **2011**, *474*, 64–67. [[CrossRef](#)] [[PubMed](#)]
47. Bao, Q.; Zhang, H.; Wang, B.B.; Ni, Z.Z.; Lim, C.H.Y.X.C.; Wang, Y.Y.; Tang, D.Y.D.; Loh, K.P. Broadband graphene polarizer. *Nat. Photon.* **2011**, *5*, 411–415. [[CrossRef](#)]
48. Luo, Z.; Zhou, M.; Weng, J.; Huang, G.; Xu, H.; Ye, C.; Cai, Z. Graphene-based passively Q-switched dual-wavelength erbium-doped fiber laser. *Opt. Lett.* **2010**, *35*, 3709–3711. [[CrossRef](#)]
49. Liu, J.; Xu, J.; Wang, P. Graphene-based passively Q-switched 2 μm thulium-doped fiber laser. *Opt. Commun.* **2012**, *285*, 5319–5322. [[CrossRef](#)]
50. Wang, Q.; Chen, T.; Zhang, B.; Li, M.; Guo, L.; Chen, K.P. All-fiber passively mode-locked thulium-doped fiber ring laser using optically deposited graphene saturable absorbers. *Appl. Phys. Lett.* **2013**, *102*, 131117. [[CrossRef](#)]
51. Wang, G.; Wang, K.; Szydłowska, B.M.; Baker-Murray, A.A.; Wang, J.-J.; Feng, Y.; Zhang, X.; Wang, J.; Blau, W.J. Ultrafast Nonlinear Optical Properties of a Graphene Saturable Mirror in the 2 μm Wavelength Region. *Laser Photon. Rev.* **2017**, *11*, 1700166. [[CrossRef](#)]
52. Wang, W.; Li, L.; Zhang, H.; Qin, J.; Lu, Y.; Xu, C.; Li, S.; Shen, Y.; Yang, W.; Yang, Y.; et al. Passively Q-switched operation of a Tm, Ho:LuVO₄ laser with a graphene saturable absorber. *Appl. Sci.* **2018**, *8*, 954. [[CrossRef](#)]
53. Steinberg, D.; Gerosa, R.M.; Pellicer, F.N.; Zapata, J.D.; Domingues, S.H.; De Souza, E.A.T.; Saito, L.A.M. Graphene oxide and reduced graphene oxide as saturable absorbers onto D-shaped fibers for sub 200-fs EDFL mode-locking. *Opt. Mater. Express* **2017**, *8*, 144–156. [[CrossRef](#)]
54. Ahmad, H.; Soltani, S.; Thambiratnam, K.; Yasin, M.; Tiu, Z. Mode-locking in Er-doped fiber laser with reduced graphene oxide on a side-polished fiber as saturable absorber. *Opt. Fiber Technol.* **2019**, *50*, 177–182. [[CrossRef](#)]
55. Yin, K.; Zhang, B.; Xue, G.; Hou, J. High-power all-fiber wavelength-tunable thulium doped fiber laser at 2 μm . *Opt. Express* **2014**, *22*, 19947–19952. [[CrossRef](#)]
56. Soltanian, M.R.K.; Ahmad, H.; Khodaie, A.; Amiri, I.; Ismail, M.F.I.M.F.; Harun, S.W. A Stable Dual-wavelength Thulium-doped Fiber Laser at 1.9 μm Using Photonic Crystal Fiber. *Sci. Rep.* **2015**, *5*, 14537. [[CrossRef](#)]
57. Zhang, Z.; Boyland, A.J.; Sahu, J.K.; Clarkson, W.A.; Ibsen, M. High-Power Single-Frequency Thulium-Doped Fiber DBR Laser at 1943 nm. *IEEE Photon. Technol. Lett.* **2011**, *23*, 417–419. [[CrossRef](#)]
58. Li, Z.; Heidt, A.M.; Daniel, J.M.O.; Jung, Y.; Alam, S.U.; Richardson, D.J. Thulium-doped fiber amplifier for optical communications at 2 μm . *Opt. Express* **2013**, *21*, 9289–9297. [[CrossRef](#)]
59. Hemming, A.; Simakov, N.; Haub, J.; Carter, A. A review of recent progress in holmium-doped silica fibre sources. *Opt. Fiber Technol.* **2014**, *20*, 621–630. [[CrossRef](#)]
60. Simakov, N.; Li, Z.; Jung, Y.; Daniel, J.M.O.; Barua, P.; Shardlow, P.C.; Liang, S.; Sahu, J.K.; Hemming, A.; Clarkson, W.A.; et al. High gain holmium-doped fibre amplifiers. *Opt. Express* **2016**, *24*, 13946–13956. [[CrossRef](#)]
61. Simakov, N.; Hemming, A.; Clarkson, W.A.; Haub, J.; Carter, A. A cladding-pumped, tunable holmium doped fiber laser. *Opt. Express* **2013**, *21*, 28415–28422. [[CrossRef](#)] [[PubMed](#)]
62. Hemming, A.; Bennetts, S.; Simakov, N.; Davidson, A.; Haub, J.; Carter, A. High power operation of cladding pumped holmium-doped silica fibre lasers. *Opt. Express* **2013**, *21*, 4560–4566. [[CrossRef](#)] [[PubMed](#)]
63. Wu, K.S.; Ottaway, D.; Munch, J.; Lancaster, D.G.; Bennetts, S.; Jackson, S.D. Gain-switched holmium-doped fibre laser. *Opt. Express* **2009**, *17*, 20872–20877. [[CrossRef](#)] [[PubMed](#)]
64. Geng, J.; Wang, Q.; Luo, T.; Case, B.; Jiang, S.; Amzajerian, F.; Yu, J. Single-frequency gain-switched Ho-doped fiber laser. *Opt. Lett.* **2012**, *37*, 3795–3797. [[CrossRef](#)]
65. Luo, H.; Liu, F.; Li, J.; Liu, Y. High repetition rate gain-switched Ho-doped fiber laser at 2.103 μm pumped by h-shaped mode-locked Tm-doped fiber laser at 1.985 μm . *Opt. Express* **2018**, *26*, 26485–26494. [[CrossRef](#)]
66. Li, P.; Ruehl, A.; Grosse-Wortmann, U.; Hartl, I. Sub-100 fs passively mode-locked holmium-doped fiber oscillator operating at 2.06 μm . *Fiber Lasers XII Technol. Syst. Appl.* **2015**, *9344*, 6859–6862. [[CrossRef](#)]

67. Chamorovskiy, A.; Marakulin, A.V.; Kurkov, A.; Okhotnikov, O.G. Tunable Ho-doped soliton fiber laser mode-locked by carbon nanotube saturable absorber. *Laser Phys. Lett.* **2012**, *9*, 602–606. [[CrossRef](#)]
68. Pawliszewska, M.; Dużyńska, A.; Zdrojek, M.; Sotor, J. Metallic carbon nanotube-based saturable absorbers for holmium-doped fiber lasers. *Opt. Express* **2019**, *27*, 11361–11369. [[CrossRef](#)]
69. Sotor, J.; Pawliszewska, M.; Sobon, G.; Kaczmarek, P.; Przewolka, A.; Pasternak, I.; Cajzl, J.; Peterka, P.; Honzátko, P.; Kašík, I.; et al. All-fiber Ho-doped mode-locked oscillator based on a graphene saturable absorber. *Opt. Lett.* **2016**, *41*, 2592–2595. [[CrossRef](#)]
70. Pawliszewska, M.; Martynkien, T.; Przewłoka, A.; Sotor, J. Dispersion-managed Ho-doped fiber laser mode-locked with a graphene saturable absorber. *Opt. Lett.* **2017**, *43*, 38–41. [[CrossRef](#)]
71. Pawliszewska, M.; Ge, Y.; Li, Z.; Zhang, H.; Sotor, J. Fundamental and harmonic mode-locking at 2.1 μm with black phosphorus saturable absorber. *Opt. Express* **2017**, *25*, 16916–16921. [[CrossRef](#)] [[PubMed](#)]
72. Chamorovskiy, A.; Marakulin, A.V.; Kurkov, A.; Leinonen, T.; Okhotnikov, O.G. High-Repetition-Rate Q-Switched Holmium Fiber Laser. *IEEE Photonics J.* **2012**, *4*, 679–683. [[CrossRef](#)]
73. Kurkov, A.; Sholokhov, E.; Marakulin, A.; Minashina, L. Dynamic behavior of laser based on the heavily holmium doped fiber. *Laser Phys. Lett.* **2010**, *7*, 587–590. [[CrossRef](#)]
74. Sholokhov, E.; Marakulin, A.; Kurkov, A.; Tsvetkov, V. All-fiber Q-switched holmium laser. *Laser Phys. Lett.* **2011**, *8*, 382–385. [[CrossRef](#)]
75. Wang, X.; Zhou, P.; Miao, Y.; Zhang, H.; Xiao, H.; Wang, X.; Liu, Z. High power, compact, passively Q-switched Ho-doped fiber laser tandem pumped by a 1150 nm Raman fiber laser. *Laser Phys. Lett.* **2014**, *11*, 095101. [[CrossRef](#)]
76. Eckmann, A.; Felten, A.; Mishchenko, A.; Britnell, L.; Krupke, R.; Novoselov, K.S.; Casiraghi, C. Probing the Nature of Defects in Graphene by Raman Spectroscopy. *Nano Lett.* **2012**, *12*, 3925–3930. [[CrossRef](#)]
77. Casiraghi, C.; Hartschuh, A.; Qian, H.; Piscanec, S.; Georgi, C.; Fasoli, A.; Novoselov, K.S.; Basko, D.M.; Ferrari, A.C. Raman Spectroscopy of Graphene Edges. *Nano Lett.* **2009**, *9*, 1433–1441. [[CrossRef](#)]
78. Shin, H.; Kim, K.K.; Benayad, A.; Yoon, S.; Park, H.K.; Jung, I.; Jin, M.H.; Jeong, H.; Kim, J.M.; Choi, J.; et al. Efficient Reduction of Graphite Oxide by Sodium Borohydride and Its Effect on Electrical Conductance. *Adv. Funct. Mater.* **2009**, *19*, 1987–1992. [[CrossRef](#)]
79. Wu, K.; Chen, B.; Zhang, X.; Zhang, S.; Guo, C.; Li, C.; Xiao, P.; Wang, J.; Zhou, L.; Zou, W.; et al. High-performance mode-locked and Q-switched fiber lasers based on novel 2D materials of topological insulators, transition metal dichalcogenides and black phosphorus: Review and perspective (invited). *Opt. Commun.* **2018**, *406*, 214–229. [[CrossRef](#)]
80. Huang, C.; Tang, Y.; Wang, S.; Zhang, R.; Zheng, J.; Xu, J. Theoretical Modeling of Ho-Doped Fiber Lasers Pumped by Laser-Diodes Around 1.125 μm . *J. Light. Technol.* **2012**, *30*, 3235–3240. [[CrossRef](#)]
81. Peterka, P.; Koška, P.; Čtyroký, J. Reflectivity of superimposed Bragg gratings induced by longitudinal mode instabilities in fiber lasers. *IEEE J. Sel. Top. Quantum Electron.* **2018**, *24*, 0902608. [[CrossRef](#)]
82. Aubrecht, J.; Peterka, P.; Koška, P.; Podrazký, O.; Todorov, F.; Honzátko, P.; Kašík, I. Self-swept holmium fiber laser near 2100 nm. *Opt. Express* **2017**, *25*, 4120–4125. [[CrossRef](#)] [[PubMed](#)]
83. Herda, R.; Kivistö, S.; Okhotnikov, O.G. Dynamic gain induced pulse shortening in Q-switched lasers. *Opt. Lett.* **2008**, *33*, 1011–1013. [[CrossRef](#)] [[PubMed](#)]